



Oleamide rescues tibialis anterior muscle atrophy of mice housed in small cages

Yasuyuki Kobayashi¹, Natsumi Watanabe¹, Tomoya Kitakaze¹, Keiichiro Sugimoto^{2,3}, Takeshi Izawa⁴, Kenji Kai¹, Naoki Harada¹ and Ryoichi Yamaji^{1*}

¹Division of Applied Life Sciences, Graduate School of Life and Environmental Sciences, Osaka Prefecture University, Sakai, Osaka 5998531, Japan

²Research and Development Center, Nagaoka Co. Ltd, Ibaraki, Osaka 5670005, Japan

³Center for Research and Development of Bioresources, Osaka Prefecture University, Sakai, Osaka 5998531, Japan

⁴Division of Veterinary Science, Graduate School of Life and Environmental Sciences, Osaka Prefecture University, Izumisano, Osaka 5988531, Japan

(Submitted 18 March 2020 – Final revision received 12 October 2020 – Accepted 27 October 2020 – First published online 4 November 2020)

Abstract

Skeletal muscle atrophy causes decreased physical activity and increased risk of metabolic diseases. We investigated the effects of oleamide (*cis*-9,10-octadecanamide) treatment on skeletal muscle health. The plasma concentration of endogenous oleamide was approximately 30 nM in male ddY mice under normal physiological conditions. When the stable isotope-labelled oleamide was orally administered to male ddY mice (50 mg/kg), the plasma concentration of exogenous oleamide reached approximately 170 nM after 1 h. Male ddY mice were housed in small cages (one-sixth of normal size) to enforce sedentary behaviour and orally administered oleamide (50 mg/kg per d) for 4 weeks. Housing in small cages decreased tibialis anterior (TA) muscle mass and the cross-sectional area of the myofibres in TA muscle. Dietary oleamide alleviated the decreases in TA muscle and resulted in plasma oleamide concentration of approximately 120 nM in mice housed in small cages. Housing in small cages had no influence on the phosphorylation levels of Akt serine/threonine kinase (Akt), mechanistic target of rapamycin (mTOR) and ribosomal protein S6 kinase (p70S6K) in TA muscle; nevertheless, oleamide increased the phosphorylation levels of the proteins. Housing in small cages increased the expression of microtubule-associated protein 1 light chain 3 (LC3)-II and sequestosome 1 (p62), but not LC3-I, in TA muscle, and oleamide reduced LC3-I, LC3-II and p62 expression levels. In C2C12 myotubes, oleamide increased myotube diameter at ≥ 100 nM. Furthermore, the mTOR inhibitor, Torin 1, suppressed oleamide-induced increases in myotube diameter and protein synthesis. These results indicate that dietary oleamide rescued TA muscle atrophy in mice housed in small cages, possibly by activating the phosphoinositide 3-kinase/Akt/mTOR signalling pathway and restoring autophagy flux.

Key words: Myotubes; Primary fatty acid amides; Mechanistic target of rapamycin signalling; Autophagy; Sedentary behaviour

Skeletal muscle is composed of myofibres and accounts for approximately 40 % of the human body weight. Postnatal skeletal muscle development occurs by muscle hypertrophy, which is accompanied by increasing the size of individual myofibre⁽¹⁾. Skeletal muscle loss occurs during immobilisation, prolonged bed rest or ageing as a result of decreased physical activity, and it causes an increased risk of developing metabolic diseases such as obesity and type 2 diabetes. Sedentary lifestyle induces low habitual physical activity, leading to a decline in the quantity and quality of skeletal muscle^(2,3). Owing to skeletal muscle's contributions to locomotion as well as to glucose and lipid metabolism, establishing methods of maintaining or enhancing skeletal muscle mass would constitute a novel therapeutic approach for restoring decreased locomotion and energy metabolism. Such an approach would consequently improve the quality of life,

regardless of age. Recently, many studies have focused on the discovery and biochemical functions of food components that are beneficial for skeletal muscle health. It is important to determine whether these food components are absorbed into the body and act on skeletal muscle at physiological concentrations.

Skeletal muscle mass depends on net protein content, which is regulated by the equilibrium between protein synthesis and degradation. The insulin-like growth factor 1 signalling pathway is a major protein synthesis pathway in the skeletal muscle. Insulin-like growth factor 1 activates the phosphoinositide 3-kinase (PI3K)/Akt serine/threonine kinase (Akt)/mechanistic target of rapamycin (mTOR) signalling pathway, which mainly controls the anabolic processes in skeletal muscle⁽⁴⁾. Phosphorylated mTOR induces the phosphorylation of downstream substrates, such as ribosomal protein S6 kinase (p70S6K), which then

Abbreviations: Akt, Akt serine/threonine kinase; CSA, cross-sectional area; DMSO, dimethyl sulfoxide; LC3, microtubule-associated protein 1 light chain 3; mTOR, mechanistic target of rapamycin; p62, sequestosome 1; p70S6K, ribosomal protein S6 kinase; PI3K, phosphoinositide 3-kinase; TA, tibialis anterior.

* **Corresponding author:** Dr Ryoichi Yamaji, fax +81 72 254 9921, email yamaji@biochem.osakafu-u.ac.jp

regulates translation initiation and capacity – the culmination of these processes eventually promotes protein synthesis. Increased protein synthesis results in myofibre hypertrophy, contributing to an increase in skeletal muscle mass. In contrast, protein degradation is mainly regulated by the ubiquitin–proteasome system and the macroautophagy (hereafter referred to as autophagy) system⁽⁵⁾. The ubiquitin–proteasome system degrades intracellular ubiquitin-conjugated proteins, and autophagy helps to clear protein aggregates and damaged or dysfunctional organelles in the cytoplasm.

Long-chain fatty acid amides are lipid mediators that function as bioactive lipid signalling molecules, and they include the primary fatty acid amides, the *N*-acylamides, the *N*-acylamino acids, the *N*-acyldopamines and the *N*-acylethanolamines⁽⁶⁾. Primary fatty acid amides could be endogenously produced and ubiquitously distributed in the body⁽⁷⁾. Oleamide (*cis*-9,10-octadecenoamide) is one of the most studied primary fatty acid amides. Oleamide induces several biological functions such as analgesic and anti-anxiety phenotypes⁽⁸⁾, sleep induction⁽⁹⁾ and anti-inflammatory activity in microglia⁽¹⁰⁾. Further novel functions of oleamide have been explored.

Oleamide has been found at concentrations of 35⁽¹¹⁾ and 57 nM⁽¹²⁾ in rat plasma and at concentrations of approximately 730–910 nM in human (males and females) plasma⁽¹³⁾. In contrast, the plasma oleamide concentration is 113 μM in luteal-phase human females⁽¹⁴⁾. Thus, the plasma concentrations of oleamide are under debate. On the other hand, oleamide is present in the essential oil of mountain celery (*Cryptotaenia japonica* Hassk) seeds and in *Penicillium candidum*-fermented dairy products (camembert cheese)^(10,15), indicating that oleamide is also a naturally occurring food component. However, it remains unclear whether orally administered oleamide is absorbed into the body.

Recently, Zhang *et al.*⁽¹⁶⁾ reported that exercise causes an increase in oleamide levels in the interstitial fluid of skeletal muscle, which suggests that oleamide may function as a signalling molecule in the skeletal muscle. Therefore, we focused on the effects of oleamide on skeletal muscle health. Sedentary lifestyle negatively affects skeletal muscle mass^(2,3). Takemura *et al.*⁽¹⁷⁾ reported that housing rodents in small cages restricts their activity and mimics sedentary behaviour, which decreases the mass of the fast-twitch plantaris muscle. In this study, we hypothesised that dietary oleamide represses skeletal muscle atrophy induced by sedentary lifestyle. The purpose of this study was to determine whether dietary oleamide is absorbed into the body and positively affects skeletal muscle atrophy at physiological concentrations, and if so, what are the underlying mechanisms? In this study, we reported that dietary stable isotope-labelled oleamide is detected in mouse plasma and that dietary oleamide has a beneficial effect on skeletal muscle atrophy in mice placed in conditions that enforce sedentary behaviour. Furthermore, we analysed the effects of oleamide on skeletal muscle health using murine C2C12 myotubes.

Materials and methods

Animals

All animals used were cared for in accordance with the guidelines of the Animal Care and Use Committee of Osaka

Prefecture University, which provided ethical approval for the present study (approval no. 30-42 and 19-207). Six-week-old healthy male Kwl:ddY mice were obtained from Kiwa Laboratory Animals (Wakayama, Japan). Mice were individually housed in normal cages (20, 12.5 and 13.0 cm height) and had free access to water and a purified diet (AIN-93G diet, in which sucrose was replaced with maize starch) during the acclimatisation period for 1 week. The mice were kept in conditions with controlled temperature (23 ± 2°C), humidity (60 ± 10%) and lighting (a 12 h light–12 h dark cycle starting at 08.00 hours) throughout the experiment.

Cell culture

Murine myoblast C2C12 cells (European Collection of Authenticated Cell Cultures) were cultured and differentiated into myotubes as previously described⁽¹⁸⁾. Briefly, myoblasts were cultured in the Dulbecco's modified Eagle's medium (Sigma-Aldrich) supplemented with 10% fetal bovine serum, 100 units/ml penicillin and 100 μg/ml streptomycin (termed growth medium). To generate myotubes, myoblasts were cultured in Dulbecco's modified Eagle's medium supplemented with 2% horse serum, 100 units/ml penicillin and 100 μg/ml streptomycin (termed differentiation medium).

Synthesis of stable isotope-labelled oleamide and heptadecenoic acid amide

[1-¹³C,¹⁵N]-Oleamide was synthesised according to the method described by Lin *et al.*⁽¹⁹⁾ except that [1-¹³C]-oleic acid and ¹⁵N-labelled ammonia hydroxide were used instead of oleic acid and ammonia hydroxide. In brief, stable isotope-labelled oleic acid (1 equiv.) (1-¹³C, 99%; Cambridge Isotope Laboratories) in dichloromethane (1 equiv.) was mixed with oxalyl chloride (1.2 equiv.) and one drop of dimethylformamide at 0°C. The mixture was allowed to react for 2 h and then concentrated using an evaporator. The resulting ¹³C-labelled oleoyl chloride (1 equiv.) in tetrahydrofuran (20 equiv.) was mixed with ¹⁵N-labelled ammonia hydroxide (3.3 N in H₂O) (98%+; Cambridge Isotope Laboratories) (10 equiv.) and stirred for 3 h. The synthesised stable isotope-labelled oleamide was purified using a reverse-phase high-performance liquid chromatography column (InertSustain C-18, 250 × 10 mm, 5-μm particle size; GL Sciences) and an isocratic mobile phase consisting of 100% acetonitrile at 40°C by monitoring at a wavelength of 210 nm. The flow rate was 4.78 ml/min. *cis*-10-Heptadecenoic acid amide was synthesised according to the method described by Lin *et al.*⁽¹⁹⁾, except that *cis*-10-heptadecenoic acid (Cayman Chemical Company) was used instead of oleic acid.

Single administration of stable isotope-labelled oleamide to mice (Expt 1)

Synthesised stable isotope-labelled oleamide was dissolved in a vehicle comprising 5% ethanol, 5% cremophor (Nacalai Tesque) and 90% saline. After 16 h of fasting, twenty-five healthy male Kwl:ddY mice (33.4 (SD 1.6) g), 7-week-old, were intragastrically administered stable isotope-labelled oleamide by using a sonde (50 mg/10 ml per kg) (CLEA Japan) (*n* 5 each time point). After administration, the plasma was collected at 0, 1, 2, 3 and 6 h



using a heparinised 1-ml glass syringe prewashed with ethanol under an anaesthesia containing three drugs (0.3 mg/kg medetomidine hydrochloride, 4 mg/kg midazolam, 5 mg/kg butorphanol tartrate, intraperitoneal).

Administration of oleamide to mice housed in small cages (Expt 2)

Eighteen healthy male Kwl:ddY mice (33.1 (SD 1.2) g), 7 weeks old, were randomly divided into three groups, termed the control group, sedentary-control group and sedentary-oleamide group (*n* 6 per group). Mice in the control group were individually housed in normal cages, and mice in the sedentary-control and sedentary-oleamide groups were individually housed in small cages (6.67, 6.25 and 13.0 cm height). Oleamide (Sigma-Aldrich), dissolved in a vehicle composed of 5% ethanol, 5% cremophor and 90% saline, was intragastrically administered to the sedentary-oleamide group by using a sonde (50 mg/10 ml/kg per d); the control group and the sedentary-control group were intragastrically administered the vehicle for 4 weeks by using a sonde. Pair-feeding was conducted to artificially match the energy intake of mice in the three groups. Mice in the sedentary-control group were fed *ad libitum*. The other two groups were fed the amount of food consumed by the sedentary-control group the previous day. All groups had free access to water during the experiments. Mice were fasted for 16 h and then administered vehicle or oleamide. After 2 h, mice were selected one by one from three experimental groups and the plasma was collected in a 1-ml glass tube using a heparinised 1-ml glass syringe under an anaesthesia containing three drugs (0.3 mg/kg medetomidine hydrochloride, 4 mg/kg midazolam, 5 mg/kg butorphanol tartrate, intraperitoneal). The glass tube and glass syringe were prewashed with ethanol. The mice were killed, the skeletal muscle tissues were excised and the extraneous tissues were cleaned off.

Concentrations of plasma oleamide and stable isotope-labelled oleamide

The blood was subjected to centrifugation at 8000 *g* for 10 min at 4°C. The supernatant (plasma sample) was stored at -80°C in a 1-ml glass tube, which had been prewashed with ethanol. Stable isotope-labelled oleamide and *cis*-10-heptadecenoic acid amide were used as an internal standard for quantitative analyses of oleamide and stable isotope-labelled oleamide, respectively. Internal standard was added to plasma sample (100 µl) and vortexed for 20 s. Ice-cold acetone (400 µl) was added to each sample, and then the sample was vortexed for 20 s and stood at -20°C for 20 min. Subsequently, the sample was subjected to centrifugation at 13 800 *g* for 10 min at 4°C, and the supernatant was evaporated with N₂ gas. Hexane (200 µl) was added to the sample, and after vortexing for 20 s, the sample was subjected to centrifugation at 3800 *g* for 5 min at 4°C and the hexane layer was removed. The sample was dissolved in ethyl acetate (300 µl) and subjected to centrifugation at 3800 *g* for 5 min at 4°C. The ethyl acetate layer was collected and fully evaporated with N₂ gas. The sample was dissolved with ethyl acetate before GC-MS analysis. The plasma samples were analysed using GCMS-QP2010 Plus (Shimadzu) and an InertCap 5MS/NP column (30 m × 0.25 mm internal diameter, 0.25 mm film, GL Sciences). The conditions were as follows:

injection volume, 1 µl (splitless mode at a 30:1 split ratio); injector temperature, 230°C; carrier gas, He (at 1.31 ml/min); transfer line temperature, 250°C; ion source temperature, 230°C and electron energy, 70 eV. The temperature of the column oven was programmed as follows: 70°C for 5 min, followed by an increase to 300°C at 10°C/min, with the temperature being maintained at 300°C for 15 min. The MS was operated by the selected ion monitoring mode for quantitative analysis (*m/z* 59, 72 for oleamide and *cis*-10-heptadecenoic acid amide; *m/z* 61, 74 for stable isotope-labelled oleamide). For Expt 1, the plasma concentrations of endogenous and exogenous oleamide were determined using five mice from each group (*n* 6 per group). For Expt 2, the plasma concentrations of endogenous oleamide were determined using five mice from each group (*n* 6 per group). The plasma sample of one mouse per each group was excluded because of technical failure to collect blood.

Grip test

The grip strength of both forelimbs was measured using a Grip Strength Meter (GPM-100; Melquest) according to the method by Takeshita *et al.*⁽²⁰⁾. The grip strength of each mouse was measured five times in succession, and the data obtained were averaged to represent the individual value for each mouse (*n* 6 per group).

Cross-sectional area

Serial cross sections (10-µm thick) were cut 3 mm from the knee of the right tibialis anterior (TA) muscle using a cryostat (Leica) at -20°C. The muscle sections were air-dried and then fixed with 10% formalin for 1 h. The sections were washed three times with PBS and incubated with PBS containing 10% normal serum and 1% Triton X-100, followed by reaction with rabbit polyclonal anti-laminin antibodies (Sigma-Aldrich). The immunoreactive sections were incubated with the secondary Alexa Fluor 488 goat anti-mouse IgG antibody (Life Technologies), and the immunofluorescent images of the muscle sections were obtained with a BIOREVO BZ-9000 microscope (Keyence). The cross-sectional area (CSA) (µm²) of myofibres was measured as previously described⁽²¹⁾. Mean fibre CSA was determined from more than 400 fibres per TA muscle (*n* 6 per group).

Histological examination of myofibres

Cross sections of the right TA muscle were cut at 10 µm using cryostat at -20°C and fixed in 10% neutral-buffered formalin. The muscle sections were then stained with haematoxylin-eosin. Histological examination was performed by a board-certified veterinary pathologist (T. I.) with a light microscope (BX-53; Olympus).

Immunofluorescence analysis

To determine the myotube diameter *in vitro*, C2C12 myoblasts were differentiated into myotubes in the differentiation medium for 6 d, followed by incubation in the presence of acetamide, lauramide, palmitamide, stearamide (Tokyo Chemical Industry), myristamide (Alfa Aesar), oleamide, oleic acid (0.1 µM each) (Fujifilm Wako) or dimethyl sulfoxide (DMSO) (vehicle) (Nacalai Tesque) for 2 d. To determine the involvement of mTOR signalling in



oleamide-induced increase in myotube diameter, myotubes were incubated with oleamide (0.1 μM) in the presence or absence of Torin 1 (0.1 μM) (Chemscone) and LY2584702 (1 μM) (Cayman Chemical Company) for 2 d. Cells were fixed in 4% paraformaldehyde in PBS, and fixed cells were analysed by immunofluorescent staining as previously described⁽²²⁾. Briefly, fixed cells were incubated with a mouse anti-MyHC antibody (clone MF20, supernatant; Developmental Studies Hybridoma Bank, University of Iowa) and then incubated with Alexa Fluor 488-conjugated goat anti-mouse IgG. Nuclei were stained with 4',6-diamidino-2-phenylindole dihydrochloride. The diameter of the short axis of myotubes was determined to evaluate myotube size, and the mean myotube diameter was determined from more than 100 myotubes for each sample as previously described⁽²²⁾.

Western blotting

Myotubes were lysed, and skeletal muscles were homogenised in lysis buffer (50 mM Tris-HCl, pH 7.5, 150 mM NaCl, 1% sodium deoxycholate, 1% Triton X-100, 0.1% SDS, 2 mM EDTA, 1 mM sodium orthovanadate, 50 mM sodium fluoride, 10 mM sodium molybdate, 10 mM sodium pyrophosphate, 1 mM dithiothreitol, 1 mM phenylmethylsulfonyl fluoride, 1 $\mu\text{g}/\text{ml}$ aprotinin and 10 $\mu\text{g}/\text{ml}$ leupeptin) and sonicated. Proteins from lysates and homogenates were subjected to SDS-PAGE and analysed by Western blotting with the following antibodies: rabbit polyclonal anti-glyceraldehyde-3-phosphate dehydrogenase⁽²³⁾, anti-Akt (Cell Signaling Technology), anti-sequestosome 1 (p62) (Medical & Biological Laboratories) and anti-histone H2B (Merck) antibodies; rabbit monoclonal anti-phospho-Akt (Ser473) (clone D9E; Cell Signaling Technology), anti-mTOR (clone 7C10; Cell Signaling Technology), anti-phospho-mTOR (Ser2448) (clone D9C2; Cell Signaling Technology), anti-p70S6K (clone 49D7; Cell Signaling Technology), anti-phospho-p70S6K (Thr389) (clone 108D2; Cell Signaling Technology), anti-atrogin-1 (clone EPR9148(2); Abcam) and anti-microtubule-associated protein 1 light chain 3 (LC3) (clone D3U4C; Cell Signaling Technology) antibodies; mouse monoclonal anti-puromycin (clone 12D9; Merck) antibodies and goat polyclonal anti-MurF-1 (R&D Systems) antibodies. Immunoreactive proteins were incubated with horseradish peroxidase-conjugated goat anti-rabbit, anti-mouse or anti-goat IgG (Bio-Rad) and subsequently treated with Super Signal West Femto Chemiluminescent Substrate (Pierce Biotechnology) or Immobilon Western Chemiluminescent horseradish peroxidase Substrate (Millipore), followed by detection with a LAS4000 imaging system (GE Healthcare).

Mechanistic target of rapamycin signalling

C2C12 myotubes were cultured in serum-free Dulbecco's modified Eagle's medium for 16 h, followed by incubation with vehicle (DMSO) or 0.1 μM oleamide for the indicated time periods. To determine the involvement of PI3K in oleamide-induced mTOR signalling activation, myotubes were incubated with oleamide (0.1 μM) or DMSO in the presence or absence of LY294002 (1 μM) (Fujifilm Wako) for 15 min.

Protein synthesis

Protein synthesis was determined as previously described⁽²⁴⁾. Briefly, C2C12 myotubes were cultured in serum-free Dulbecco's

modified Eagle's medium for 16 h, followed by incubation with oleamide (0.1 μM) or DMSO in the presence or absence of Torin 1 (0.1 μM) for 1 h. After stimulation with oleamide, the myotubes were incubated with puromycin at a final concentration of 1 $\mu\text{g}/\text{ml}$ for 20 min.

Statistical analysis

For *in vivo* experiments, three primary outcome measures were analysed: grip strength, skeletal muscle mass and CSA. In addition, three secondary outcome measures were evaluated: mTOR signalling-related protein expression, autophagy-related protein expression and E3 ubiquitin ligase expression. For *in vitro* experiments, one primary outcome measure was analysed: myotube diameter. In addition, four secondary outcome measures were evaluated: protein synthesis, mTOR signalling-related protein expression, autophagy-related protein expression and E3 ubiquitin ligase expression.

Data were verified for normal distribution using the Shapiro-Wilk test before parametric analyses. One-way ANOVA followed by Dunnett's *post hoc* test or two-way ANOVA followed by Tukey's *post hoc* test was used to analyse data from the experiments with three or more groups. Significant differences between two groups – the control group *v.* the sedentary-control group, and the sedentary-control group *v.* the sedentary-oleamide group – in the animal experiments were determined using Student's *t* test. The number of mice per group for detecting a significant difference between groups (main parameter: skeletal muscle weight) was calculated by G*Power (3.1.9.4) assuming a hypothesised effect size of 2.7, an error of 0.05 (two-tail) and a statistical power of 0.95. The calculations were based on a previous study⁽¹⁷⁾. For *in vivo* experiments, '*n*' refers to the number of individual mice in each group and *n* is six unless indicated otherwise. For *in vitro* experiments, '*n*' refers to the number of individual dishes or wells in each group and *n* is three unless indicated. Statistical analysis was performed using JMP statistical software version 8.0.1 (SAS Institute). Data are presented as mean values and standard deviations. Differences were considered statistically significant at $P < 0.05$.

Results

Plasma concentrations of oleamide before and after oleamide administration

The plasma concentration of oleamide was 30.4 (SD 13.3) nM in 7-week-old male ddY mice (Fig. 1(a)). When the stable isotope-labelled oleamide was orally administered to ddY mice, the plasma concentration of exogenous oleamide reached approximately 170 nM by 1 h after single-dose administration and was maintained at that concentration until 6 h after oral administration (Fig. 1(b)).

Dietary oleamide restores tibialis anterior muscle atrophy in mice housed in small cages

Preliminary experiments demonstrated that the food consumption of mice housed in small cages may reduce compared with that of mice housed in normal cages (online Supplementary Fig. S1). Therefore, pair-feeding was conducted to artificially match the energy intake of



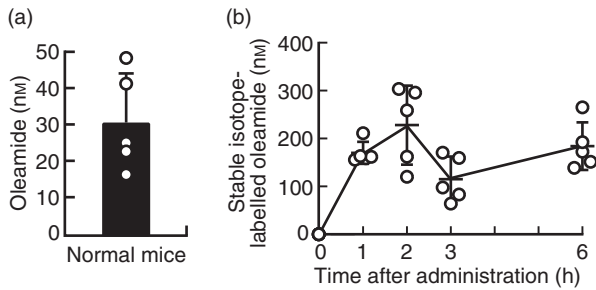


Fig. 1. Plasma concentrations of endogenous and exogenous oleamide. (a) Plasma concentrations of endogenous oleamide in mice. Values are means and standard deviations (n 5). (b) Plasma concentrations of exogenous oleamide after oral administration of stable isotope-labelled oleamide. Values are means and standard deviations (n 5 per each time point).

mice. There was no significant difference between the control group and the sedentary-control group and between the sedentary-control group and the sedentary-oleamide group, with regard to the body weight (Table 1). Housing mice in small cages induced loss of TA muscle mass, and dietary oleamide alleviated the decreases of TA muscle mass in mice housed in small cages. Housing in small cages or dietary oleamide did not influence the muscle mass of gastrocnemius, plantaris or extensor digitorum longus muscles, and the fat mass of mesenteric or inguinal fat. In the TA muscle, the CSA of each muscle fibre was assessed using immunofluorescent labelling with anti-laminin antibody (Fig. 2(a)). The frequency distribution of fibre CSA shifted towards smaller sizes in the sedentary-control group compared with the control group and towards larger sizes in the sedentary-oleamide group compared with the sedentary-control group (Fig. 2(b)). Housing in small cages led to a decrease in the size of TA muscle fibre CSA, and dietary oleamide attenuated the decrease in CSA of mice housed in small cages ($P < 0.05$; Fig. 2(c)). In addition, the TA muscle sections from the three groups tested were examined histopathologically (Fig. 2(d)). There were no histological abnormalities such as degeneration/necrosis of the myofibres, increased central nuclei and inflammatory cell infiltrate in the three groups. Grip strength was significantly decreased in the sedentary-control group (1.48 (SD 0.08) N) compared with the control group (1.99 (SD 0.13) N) (Fig. 2(e)). Dietary oleamide attenuated the decrease in grip strength of mice housed in small cages (1.63 (SD 0.08) N). The plasma

concentrations of oleamide were approximately 40 nM in the control group and the sedentary-control group, and there was no significant difference between these two groups ($P < 0.05$; Fig. 3). Dietary oleamide significantly increased the plasma concentration of oleamide to approximately 120 nM in mice housed in small cages.

Oleamide activates Akt/mechanistic target of rapamycin signalling in tibialis anterior muscle of mice housed in small cages

The ratio of the levels of Akt, mTOR and p70S6K to that of histone H2B level in TA muscle was not significantly different between the control group and the sedentary-control group and between the sedentary-control group and the sedentary-oleamide group (Fig. 4, middle panels). The ratio of phosphorylation level:the respective total level of Akt, mTOR and p70S6K proteins in TA muscle was not significantly different between the control group and the sedentary-control group, whereas oleamide administration significantly increased the ratio in mice housed in small cages ($P < 0.05$; Fig. 4, lower panels).

Dietary oleamide decreases the expression levels of LC3-II and p62 in tibialis anterior muscles of mice housed in small cages

Housing in small cages increased the expression levels of LC3-II, a marker of autophagy, and p62, a selective substrate of autophagy, but not of LC3-I, in TA muscle ($P < 0.05$; Fig. 5). Dietary oleamide reduced LC3-I, LC3-II and p62 expression in the mice housed in small cages ($P < 0.05$). Moreover, housing in small cages had no influence on the expression levels of atrogin-1 and MuRF1, which are E3 ubiquitin ligases, and dietary oleamide increased atrogin-1 ($P < 0.05$), but not muscle ring-finger protein-1 (MuRF1), expression in mice placed in small cages.

Oleamide induces hypertrophy in C2C12 myotubes

C2C12 myotubes were cultured in the presence of oleamide for 2 d and were fluorescently labelled using primary anti-MyHC antibody and fluorescent secondary antibody, followed by 4',6-diamidino-2-phenylindole dihydrochloride nuclear staining (Fig. 6(a)). Oleamide increased the short axis diameters of

Table 1. Body weight and skeletal muscle mass in oleamide-fed sedentary mice (Mean values and standard deviations)

Weight	Control group		Sedentary group			
	Vehicle (n 6)		Vehicle (n 6)		Oleamide (n 6)	
	Mean	SD	Mean	SD	Mean	SD
Body weight (g)	35.5	3.9	34.5	3.3	35.3	1.5
Soleus (mg)	13.7	1.9	15.5	2.0	13.5	3.3
Gastrocnemius (mg)	310.3	33.7	290.1	29.4	313.9	14.9
Plantaris (mg)	36.7	4.1	34.1	5.1	36.3	3.0
Tibialis anterior (mg)	107.9*	7.5	96.1	7.9	110.0*	6.4
Extensor digitorum longus (mg)	22.5	2.6	20.9	3.6	22.1	0.9
Quadriceps femoris (mg)	490.4	52.8	474.0	36.3	501.5	19.6
Mesenteric fat (mg)	273.0	121.1	151.7	94.3	194.2	41.4
Inguinal fat (mg)	584.1	189.4	445.9	101.2	469.5	110.2

* The statistical significance of the differences between the control group and sedentary-control group and between the sedentary-control group and sedentary-oleamide group was analysed using Student's t test ($P < 0.05$ v. sedentary-control group).

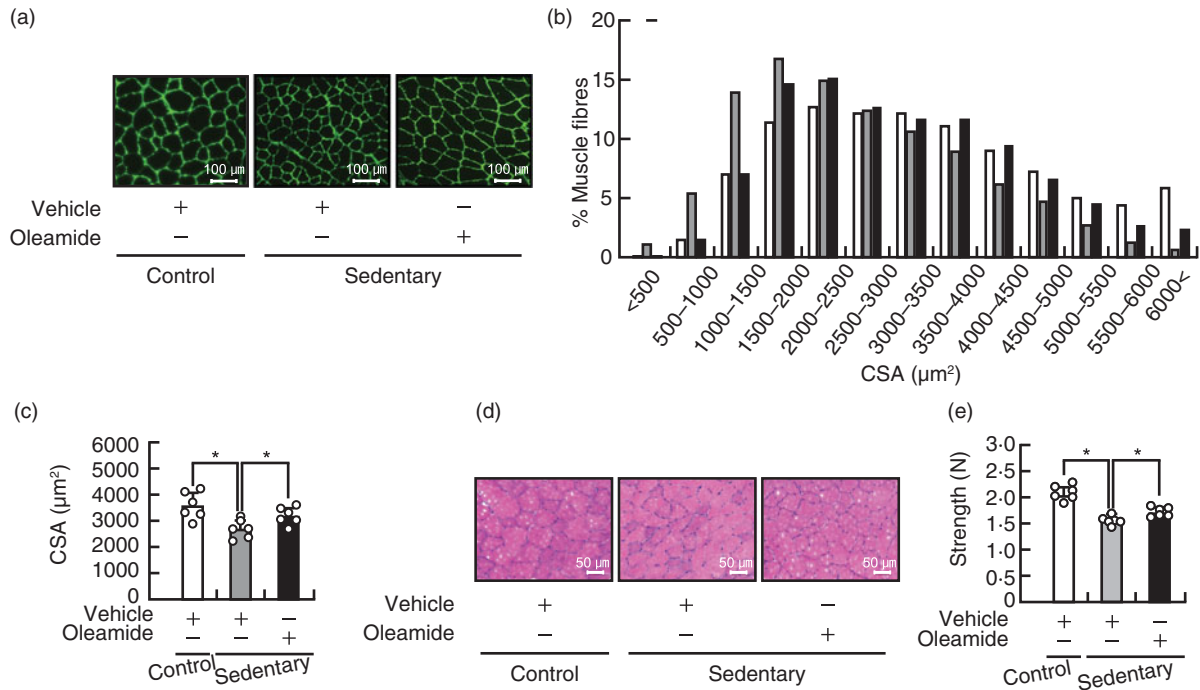


Fig. 2. Effects of dietary oleamide on muscle atrophy of mice housed in small cages. (a) Immunofluorescent staining of laminin on transverse sections of the tibialis anterior (TA) muscle. Each image is representative of a TA muscle from each group. Scale bar: 100 μm. (b) Distribution of TA muscle fibre cross-sectional area (CSA). □, Control-vehicle; ▒, sedentary-vehicle; ■, sedentary-oleamide. (c) Average size of TA muscle fibre CSA. Values are means and standard deviations (*n* 6). (d) Haematoxylin and eosin staining of the TA muscle. Each image is representative of a TA muscle from each group. Scale bar: 50 μm. (e) Grip strength. Values are means and standard deviations (*n* 6). The statistical significance of the differences between the control group and sedentary-control group and between the sedentary-control group and sedentary-oleamide group was analysed using Student's *t* test (**P* < 0.05).

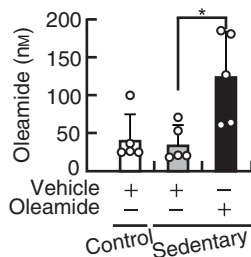


Fig. 3. Plasma concentrations of oleamide in oleamide-fed sedentary mice. Values are means and standard deviations (*n* 5). The statistical significance of the differences between the control group and the sedentary-control group and between the sedentary-control group and the sedentary-oleamide group was analysed using Student's *t* test (**P* < 0.05 v. sedentary-control group).

myotubes at concentrations of 0.1 μM or higher (*P* < 0.05), but oleic acid had no influence on the myotube diameter at a concentration of 0.1 μM (Fig. 6(b)). Furthermore, C2C12 myotubes were cultured in the presence of various primary fatty acid amides for 2 d and were fluorescently labelled (Fig. 6(c)). C2C12 myotube hypertrophy was induced by stearamide at 0.1 μM (*P* < 0.05), but not by acetamide, lauramide, myristamide and palmitamide (Fig. 6(d)). Oleamide significantly increased the phosphorylation levels of Akt, mTOR and p70S6K in C2C12 myotubes (*P* < 0.05; Fig. 6(e)). Next, C2C12 myotubes were cultured with oleamide in the presence and absence of the p70S6K inhibitor LY2584702 and were fluorescently labelled (Fig. 6(f)). LY2584702 inhibited oleamide-induced increase in

myotube size (*P* < 0.05; Fig. 6(g)). In addition, C2C12 myotubes were cultured with oleamide in the presence and absence of the mTOR inhibitor Torin 1 and were fluorescently labelled (Fig. 6(h)). Torin 1 inhibited oleamide-induced increase in myotube size (*P* < 0.05; Fig. 6(i)). Similarly, oleamide increased protein synthesis, and Torin 1 inhibited the increase (*P* < 0.05; Fig. 6(j)). LY294002, a PI3K inhibitor, inhibited oleamide-induced p70S6K phosphorylation (*P* < 0.05; Fig. 6(k)). However, oleamide had no influence on the protein levels of LC3-I, LC-II, p62, atrogin 1 and MuRF1 (Fig. 6(l)).

Discussion

Oleamide is a lipid mediator with several biological activities, and further novel effects of oleamide are being explored. Oleamide is present in the plasma in the nanomolar range or in the micromolar range⁽¹¹⁻¹³⁾, and the plasma concentrations of oleamide are still under debate. Recently, oleamide was detected in the interstitial fluid of the skeletal muscle after exercise⁽⁴⁶⁾. In this study, we investigated plasma oleamide concentrations before and after the administration of a single dose of stable isotope-labelled oleamide. Further, to determine the novel effects of oleamide on skeletal muscle health, we assessed whether oleamide has the potential to repress muscle atrophy in mice housed in small cages.

The plasma concentration of endogenous oleamide was approximately 30 nm in normal mice, almost consistent with previous reports^(11,12) that the plasma concentrations of oleamide

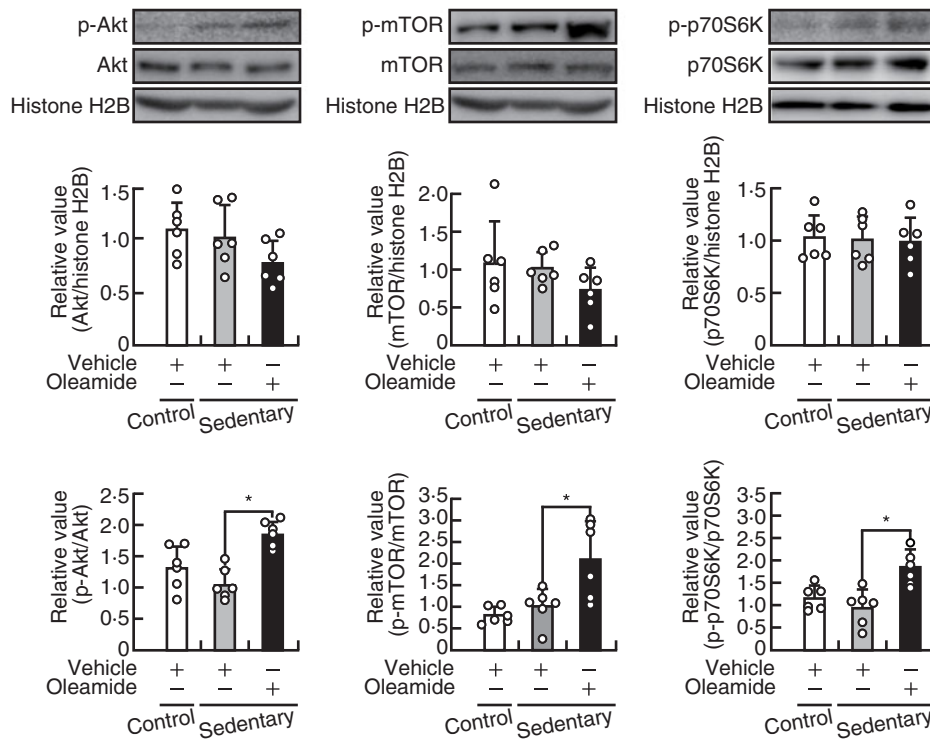


Fig. 4. Effects of oleamide on the Akt serine/threonine kinase (Akt)/mechanistic target of rapamycin (mTOR) signalling pathway in tibialis anterior (TA) muscles of mice housed in small cages. TA muscle protein Western blots; the protein levels of Akt, mTOR and ribosomal protein S6 kinase (p70S6K) were normalised to that of histone H2B, and phosphorylation levels of Akt, mTOR and p70S6K were normalised to the level of the respective protein. Values are means and standard deviations (n 6). The statistical significance of the differences between the control group and sedentary-control group and between the sedentary-control group and sedentary-oleamide group was analysed using Student's t test ($*P < 0.05$).

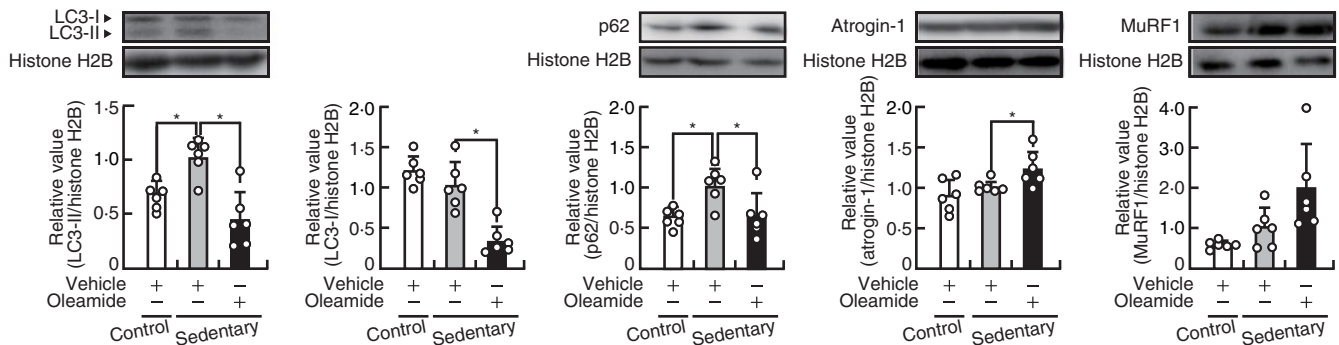


Fig. 5. Effects of dietary oleamide on autophagy- and ubiquitin-proteasome-related protein expression in tibialis anterior (TA) muscle of mice housed in small cages. TA muscle protein Western blots; each protein level was normalised to histone H2B level. Values are means and standard deviations (n 6). The statistical significance of the differences between the control group and sedentary-control group and between the sedentary-control group and sedentary-oleamide group was analysed using Student's t test ($*P < 0.05$). LC3, microtubule-associated protein 1 light chain 3; p62, sequestosome 1; MuRF1, muscle ring-finger protein-1.

are approximately 35 and 57 nM in normal rats. By contrast, oleamide is detected at higher concentrations of approximately 205–255 ng/ml (730–910 nM) in healthy human plasma⁽¹³⁾ and of approximately 113 μ M in luteal-phase human females⁽¹⁴⁾. Therefore, the plasma concentrations of oleamide may vary depending on physiological or pathophysiological conditions. On the other hand, oleamide could be leached into contact solvents from plastic labware and also non-plastic labware such as glass vial inserts⁽²⁵⁾. Contamination of plastic and non-plastic labware-derived oleamide should be taken into consideration in the

quantitative analysis of oleamide. We quantitatively measured the plasma concentrations of oleamide with minimised contamination from labwares by using ethanol-washed glass labware during the experiments. In contrast, healthy human plasma samples are prepared by mixing plasma with 50% acetone–acetonitrile in 1.5-ml Eppendorf tubes⁽¹³⁾. Therefore, the oleamide concentrations of approximately 730–910 nM in human plasma may contain labware-derived oleamide. In addition, in this study, the stable isotope-labelled oleamide was used to determine the concentration of exogenous oleamide. In Fig. 1(b),

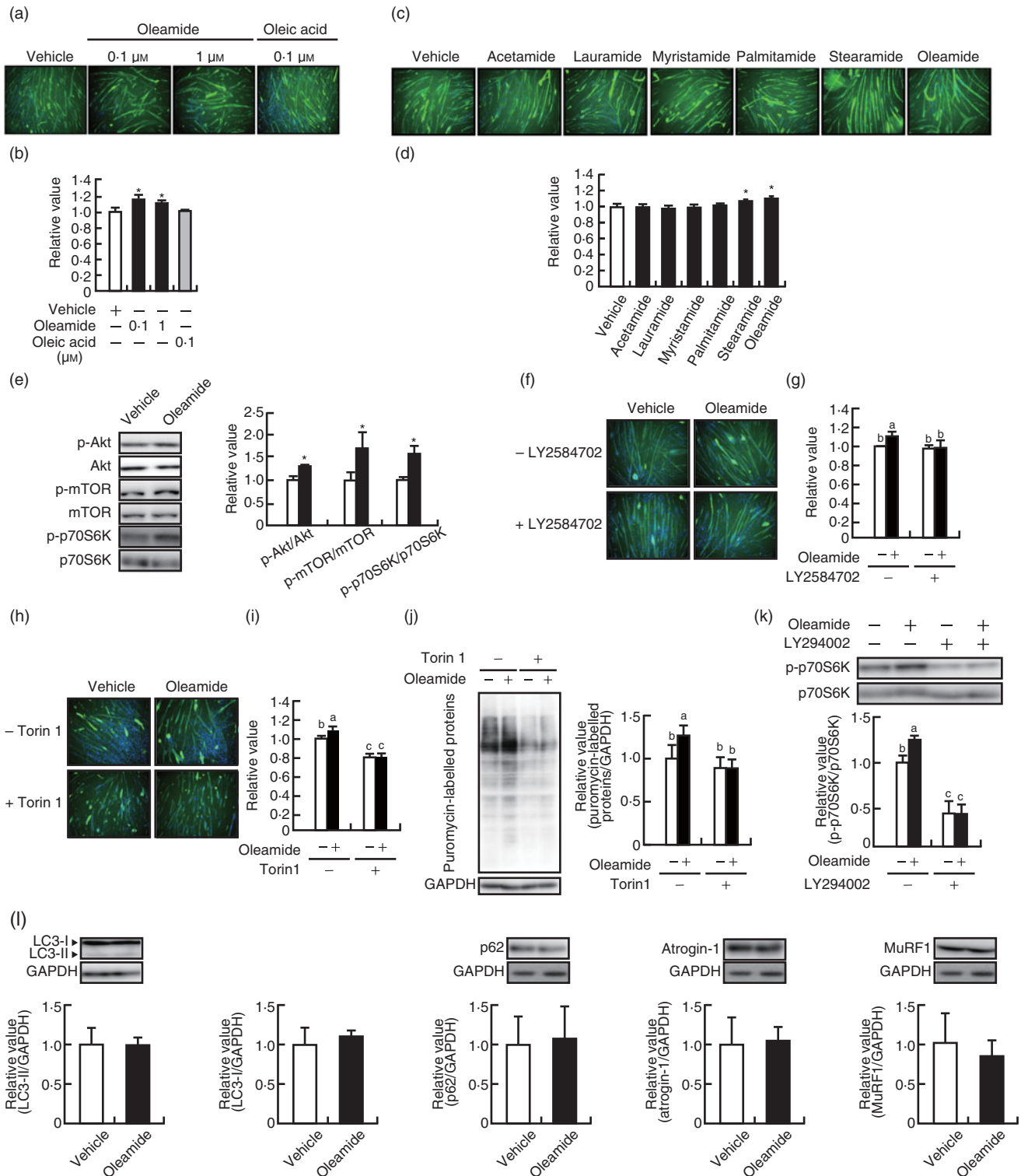


Fig. 6. Involvement of the phosphoinositide 3-kinase (PI3K)/Akt serine/threonine kinase (Akt)/mechanistic target of rapamycin (mTOR) signalling pathway in oleamide-induced hypertrophy in C2C12 myotubes. (a) Representative immunofluorescent images; C2C12 myotubes were cultured in the presence of the vehicle, oleamide or oleic acid. (b) The myotube diameters were measured. (c) Representative immunofluorescent images; C2C12 myotubes were cultured in the presence of the vehicle (DMSO), acetamide, lauramide, myristamide, palmitamide, stearamide and oleamide. (d) The myotube diameters were measured. (e) Cell lysate Western blots; C2C12 myotubes were stimulated with oleamide. Phosphorylated protein level was normalised to the respective total protein level. (f) Representative immunofluorescent images; C2C12 myotubes were cultured with oleamide in the presence or absence of LY2584702. (g) The myotube diameter was measured. (h) Representative immunofluorescent images; C2C12 myotubes were cultured with oleamide in the presence or absence of Torin 1. (i) The myotube diameter was measured. (j) Western blot of puromycin-labelled proteins; C2C12 myotubes were cultured with oleamide in the presence or absence of Torin 1, followed by incubation with puromycin. Puromycin-labelled protein levels were normalised to anti-glyceraldehyde 3-phosphate dehydrogenase (GAPDH) level. (k) Cell lysate Western blots; C2C12 myotubes were incubated with oleamide in the presence or absence of LY294002. Phosphorylated protein level was normalised to the respective total protein level. (l) C2C12 myotubes were cultured with oleamide. Each protein level was normalised to GAPDH level. For (b) and (d), values are means and standard deviations (n 4), and * indicates $P < 0.05$ v. the vehicle based on the results of a one-way ANOVA with Dunnett's *post hoc* test. For (e) and (l), values are means and standard deviations (n 4), and * indicates $P < 0.05$ v. the vehicle based on the results of Student's *t* test. For (i), (j) and (k), values are means and standard deviations (n 4). ^{a,b,c} Unlike letters indicate statistically significant differences, determined by two-way ANOVA and Tukey's *post hoc* test. □, Vehicle; ■, oleamide. LC3, microtubule-associated protein 1 light chain 3; p62, sequestosome 1; MuRF1, muscle ring-finger protein-1.

mice were individually housed in normal cages during the acclimatisation period for 1 week. After 16 h of fasting, mice were intragastrically administered the stable isotope-labelled oleamide and kept in normal cages. The plasma concentration of exogenous oleamide was approximately 170 nM 1 h after a single dose of stable isotope-labelled oleamide (50 mg/10 ml per kg). The sum of the endogenous oleamide and exogenous oleamide was approximately 200 nM. In Fig. 3, mice were individually housed in small cages for 4 weeks. After 16 h of fasting, mice were intragastrically administered oleamide (50 mg/kg per d) and kept in small cages. The plasma concentration of oleamide was approximately 120 nM. These differences in plasma oleamide concentrations may be due to the difference in the conditions under which the mice were housed. Thus, oleamide absorption may be reduced in mice housed in small cages for 4 weeks. Taken together, the plasma concentrations of oleamide were in the nanomolar range, even when mice were administered oleamide (50 mg/kg per d).

Stearamide also induced myotube hypertrophy at a concentration of 0.1 μ M in C2C12 myotubes. In healthy human plasma, stearamide is detected at concentrations of approximately 85–140 ng/ml (300–495 nM)⁽¹³⁾. As stearamide could also be leached into contact solvents from the plastic and non-plastic labwares⁽²⁵⁾, their labwares should not be used for the preparation of plasma stearamide. We found that stearamide also activated mTOR signalling (data not shown). These results suggest that stearamide has beneficial effects on skeletal muscle health via the same molecular mechanism as oleamide. In the interstitial fluid of skeletal muscle after exercise, oleamide level is increased, but there is no information on stearamide level⁽¹⁶⁾. Therefore, in this study, we focused on oleamide rather than stearamide.

In C2C12 myotubes, oleamide, but not oleic acid, induced hypertrophy at a concentration (100 nM) comparable with the physiological concentration of oleamide in the plasma of the sedentary-oleamide group. Myotube size is regulated by the balance between protein synthesis and protein degradation. Insulin-like growth factor 1 induces myotube hypertrophy by activating the PI3K/Akt/mTOR signalling pathway and by promoting protein synthesis⁽⁴⁾. Oleamide stimulated the phosphorylation of Akt, mTOR and p70S6K in C2C12 myotubes. Furthermore, LY294002 inhibited oleamide-activated p70S6K phosphorylation, and Torin 1 and LY2584702 inhibited oleamide-induced myotube hypertrophy. The activating effects of oleamide on Akt/mTOR signalling were reflected in the fast-twitch TA muscles of mice housed in small cages to enforce sedentary behaviour. These results suggest that oleamide induces hypertrophy by promoting protein synthesis through the activation of the PI3K/Akt/mTOR signalling pathway in C2C12 myotubes and represses atrophy through the activation of the PI3K/Akt/mTOR signalling pathway in the TA muscle of mice placed in small cages.

The restricted condition of the small cages increased p62 and LC3-II, but not LC3-I, expression in mice TA muscles, and dietary oleamide repressed these increases. Autophagy is necessary to expel damaged proteins and organelles. Excessive activation of autophagy causes skeletal muscle atrophy⁽²⁶⁾, whereas autophagy inhibition by muscle-specific deletion of a crucial autophagy gene, Atg7, increases the accumulation of p62 and

LC3-I in skeletal muscle, which consequently induces skeletal muscle atrophy and age-dependent decrease in muscle force⁽²⁷⁾. Atg7 is involved in the conversion of LC3-I to LC3-II. Therefore, housing in small cages may repress autophagy downstream of the LC3-I/LC3-II conversion. Autophagy inhibition aggravates skeletal muscle atrophy in catabolic conditions, such as denervation and fasting. Furthermore, in skeletal muscle, ageing leads to the accumulation of p62 and LC3-II in mice⁽²⁸⁾, suggesting that inefficient autophagy flux contributes to muscle atrophy. In this study, oleamide inhibited p62 and LC3-II accumulation, which increased due to sedentary conditions simulated by housing the mice in small cages. Thus, the results of this study suggest that oleamide contributes to the maintenance of skeletal muscle mass, possibly by restoring autophagy flux during muscle atrophy in mice housed in small cages. However, only the assessment of static LC3II and p62 protein expression leads to misinterpretation of autophagy flux. Further studies are necessary to evaluate the autophagy flux.

Traditional approaches for reducing physical activity in rodent models include denervation and hindlimb suspension^(29,30). The ankle joints are extended after denervation or during unloading, leading to a passive shortening of ankle plantarflexors (e.g. gastrocnemius, soleus and plantaris muscles)^(31–33). Since force production is low under such conditions, the plantarflexors may be more susceptible to atrophy than the dorsiflexors (e.g. TA muscle). These models are not suitable as models for reducing physical activity due to sedentary lifestyle because they drastically disrupt the ability of rodents to ambulate. Takemura *et al.*⁽¹⁷⁾ examined the effects of restricted activity on the properties of the slow and fast plantarflexor muscles in rats. Housing rats in small cages causes restricted activity and reduces muscle mass of fast-twitch plantaris muscle. In contrast, in this study, housing mice in small cages resulted in muscle atrophy of fast-twitch TA muscle, but not of plantaris muscle. Restricted activity by housing in small cages had no influence on slow-twitch soleus muscle in rats and mice. These results indicate that the restricted activity due to sedentary lifestyles affects fast-twitch muscles more than slow-twitch muscles. When mice are housed in small cages, they remain sedentary. Under sedentary conditions, plantaris and soleus muscles of mice are maintained in a stretched state and TA muscle is maintained in a contracted state. Therefore, we suggest that muscle atrophy is prominent in the TA muscle of mice housed in small cages.

In C2C12 myotube cells, oleamide activated the mTOR signalling, consistent with results from animal models. However, oleamide did not affect autophagy in C2C12 myotubes, inconsistent with results from animal models. Thus, activation of mTOR signalling by oleamide was a common phenomenon in both *in vitro* and *in vivo* models. Activation of mTOR signalling induces skeletal muscle hypertrophy and prevents skeletal muscle atrophy⁽⁴⁾. Considering the replacement of the use of animals in research, C2C12 myotubes would be utilised as a model for the mechanism of activation of mTOR signalling by oleamide.

Exercise increases oleamide levels in the interstitial fluid of skeletal muscle by >3-fold⁽¹⁶⁾. The physiological significance of exercise-induced increase in oleamide in the interstitial fluid of skeletal muscle remains unclear. Because exercise is important for the maintenance and enhancement of skeletal muscle mass, exercise-induced increase in endogenous oleamide may

help to promote skeletal muscle hypertrophy in an autocrine manner. In this study, we demonstrated that dietary oleamide may serve as a promising compound to combat TA muscle atrophy induced by sedentary behaviour in mice. Regarding the promise of oleamide for preventing or ameliorating skeletal muscle mass loss due to sedentary behaviour in humans, it would be important to identify target proteins for oleamide to activate mTOR signalling at the cellular level (e.g. C2C12 myotubes). Furthermore, the results of this study could serve as fundamental data for further studies on the efficiency of oleamide against skeletal muscle atrophy induced by different factors such as immobilisation, prolonged bed rest or ageing in humans.

Acknowledgements

We would like to thank Editage (www.editage.jp) for English language editing.

This work was supported by a Grant-in-Aid for Scientific Research from the Japan Society for the Promotion of Science (grant number 20K21285, to R. Y.), by a Grant-in-Aid from the Food Science Institute Foundation (Ryoushoku-kenkyukai) (grant number 2019A12, to R. Y.) and by research funds from Nagaoka Co. Ltd.

The authors' contributions were as follows: Y. K. and R. Y. designed the research; Y. K., N. W., T. K. and T. I. conducted the research; Y. K., N. W. and K. K. conducted GC-MS analysis; Y. K., K. S., K. K., N. H. and R. Y. analysed the data; Y. K. and R. Y. wrote the paper and R. Y. had primary responsibility for the final content.

K. S. is an employee of Nagaoka Co. Ltd.

Supplementary material

For supplementary material referred to in this article, please visit <https://doi.org/10.1017/S0007114520004304>

References

- Gokhin DS, Ward SR, Bremner SN, *et al.* (2008) Quantitative analysis of neonatal skeletal muscle functional improvement in the mouse. *J Exp Biol* **211**, 837–843.
- Rudrappa SS, Wilkinson DJ, Greenhaff PL, *et al.* (2016) Human skeletal muscle disuse atrophy: effects on muscle protein synthesis, breakdown, and insulin resistance—a qualitative review. *Front Physiol* **7**, 361.
- Hamilton MT (2018) The role of skeletal muscle contractile duration throughout the whole day: reducing sedentary time and promoting universal physical activity in all people. *J Physiol* **596**, 1331–1340.
- Bodine SC, Stitt TN, Gonzalez M, *et al.* (2001) Akt/mTOR pathway is a crucial regulator of skeletal muscle hypertrophy and can prevent muscle atrophy *in vivo*. *Nat Cell Biol* **11**, 1014–1019.
- Varshavsky A (2017) The ubiquitin system, autophagy, and regulated protein degradation. *Annu Rev Biochem* **86**, 123–128.
- Farrell EK & Merkle DJ (2008) Biosynthesis, degradation and pharmacological importance of the fatty acid amides. *Drug Discov Today* **13**, 558–568.
- Divito EB & Cascio M (2013) Metabolism, physiology, and analyses of primary fatty acid amides. *Chem Rev* **113**, 7343–7353.
- Fedorova I, Hashimoto A, Fecik RA, *et al.* (2001) Behavioral evidence for the interaction of oleamide with multiple neurotransmitter systems. *J Pharmacol Exp Ther* **299**, 332–342.
- Cravatt BF, Prospero-Garcia O, Siuzdak G, *et al.* (1995) Chemical characterization of a family of brain lipids that induce sleep. *Science* **268**, 1506–1509.
- Ano Y, Ozawa M, Kutsukake T, *et al.* (2015) Preventive effects of a fermented dairy product against Alzheimer's disease and identification of a novel oleamide with enhanced microglial phagocytosis and anti-inflammatory activity. *PLOS ONE* **10**, e0118512.
- Hanuš LO, Fales LO, Spande TF, *et al.* (1999) A gas chromatographic-mass spectral assay for the quantitative determination of oleamide in biological fluids. *Anal Biochem* **270**, 159–166.
- Chaturvedi S, Driscoll WJ, Elliot BM, *et al.* (2006) *In vivo* evidence that *N*-oleoylglycine acts independently of its conversion to oleamide. *Prostaglandins Other Lipid Mediat* **81**, 136–149.
- Castillo-Peinado LS, López-Bascón MA, Mena-Bravo A, *et al.* (2019) Determination of primary fatty acid amides in different biological fluids by LC-MS/MS in MRM mode with synthetic deuterated standards: influence of biofluid matrix on sample preparation. *Talanta* **193**, 29–36.
- Arafat ES, Trimble JW, Andersen RN, *et al.* (1989) Identification of fatty acid amides in human plasma. *Life Sci* **45**, 1679–1687.
- Cheng MC, Ker YB, Yu TH, *et al.* (2010) Chemical synthesis of 9(*Z*)-octadecenamide and its hypolipidemic effect: a bioactive agent found in the essential oil of mountain celery seeds. *J Agric Food Chem* **58**, 1502–1508.
- Zhang J, Bhattacharyya S, Hickner RC, *et al.* (2019) Skeletal muscle interstitial fluid metabolomics at rest and associated with an exercise bout: application in rats and humans. *Am J Physiol Endocrinol Metab* **316**, 43–53.
- Takemura A, Roy RR, Edgerton VR, *et al.* (2016) Biochemical adaptations in a slow and a fast plantarflexor muscle of rats housed in small cages. *Aerosp Med Hum Perform* **87**, 443–448.
- Ogawa M, Yamaji R, Higashimura Y, *et al.* (2011) 17 β -Estradiol represses myogenic differentiation by increasing ubiquitin-specific peptidase 19 through estrogen receptor α . *J Biol Chem* **286**, 41455–41465.
- Lin H, Long JZ, Roche AM, *et al.* (2018) Discovery of hydrolysis-resistant isoindoline *N*-acyl amino acid analogues that stimulate mitochondrial respiration. *J Med Chem* **61**, 3224–3230.
- Takeshita H, Yamamoto K, Nozato S, *et al.* (2017) Modified forelimb grip strength test detects aging-associated physiological decline in skeletal muscle function in male mice. *Sci Rep* **7**, 42323.
- Kitakaze T, Harada N, Imagita H, *et al.* (2015) β -Carotene increases muscle mass and hypertrophy in the soleus muscle in mice. *J Nutr Sci Vitaminol (Tokyo)* **61**, 481–487.
- Kitakaze T, Sakamoto T, Kitano T, *et al.* (2016) The collagen derived dipeptide hydroxyprolyl-glycine promotes C2C12 myoblast differentiation and myotube hypertrophy. *Biochem Biophys Res Commun* **478**, 1292–1297.
- Yamaji R, Fujita K, Takahashi S, *et al.* (2003) Hypoxia up-regulates glyceraldehyde-3-phosphate dehydrogenase in mouse brain capillary endothelial cells: involvement of Na⁺/Ca²⁺ exchanger. *Biochim Biophys Acta* **1593**, 269–276.
- Ono S, Yoshida N, Maekawa D, *et al.* (2018) 5-Hydroxy-7-methoxyflavone derivatives from *Kaempferia parviflora* induce skeletal muscle hypertrophy. *Food Sci Nutr* **7**, 312–321.
- Jug U, Naumoska K, Metličar V, *et al.* (2020) Interference of oleamide with analytical and bioassay results. *Sci Rep* **10**, 2163.



26. Zhao J, Brault JJ, Schild A, *et al.* (2007) FoxO3 coordinately activates protein degradation by the autophagic/lysosomal and proteasomal pathways in atrophying muscle cells. *Cell Metab* **6**, 472–483.
27. Masiero E, Agatea L, Mammucari C, *et al.* (2009) Autophagy is required to maintain muscle mass. *Cell Metab* **10**, 507–515.
28. Chang YC, Chen YT, Liu HW, *et al.* (2019) Oligonol alleviates sarcopenia by regulation of signaling pathways involved in protein turnover and mitochondrial quality. *Mol Nutr Food Res* **63**, 1801102.
29. Ogawa M, Kariya Y, Kitakaze T, *et al.* (2013) The preventive effect of β -carotene on denervation-induced soleus muscle atrophy in mice. *Br J Nutr* **109**, 1349–1358.
30. Haida N, Fowler WM Jr, Abresch RT, *et al.* (1989) Effect of hindlimb suspension on young and adult skeletal muscle. I. Normal mice. *Exp Neurol* **103**, 68–76.
31. Riley DA, Ellis S, Giometti J, *et al.* (1992) Muscle sarcomere lesions and thrombosis after spaceflight and suspension unloading. *J Appl Physiol* **73**, 33–43.
32. Kawano F, Ishihara J, Stevens L, *et al.* (2004) Tension- and afferent input-associated responses of neuromuscular system of rats to hindlimb unloading and/or tenotomy. *Am J Physiol Regul Integr Comp Physiol* **287**, 76–86.
33. Ohira M, Hanada H, Kawano F, *et al.* (2002) Regulation of the properties of rat hind limb muscles following gravitational unloading. *Jpn J Physiol* **52**, 235–245.